A Theoretical Determination of the Low-lying Electronic States of the *p*-Benzosemiquinone Radical Anion

Rosendo Pou-Amérigo,* Luis Serrano-Andrés, Manuela Merchán, Enrique Ortí, and Niclas Forsberg

Contribution from the Departament de Química Física, Universitat de València, Dr. Moliner, 50 E-46100 Burjassot (València), Spain, and Department of Theoretical Chemistry, Chemical Center, University of Lund, POB 124 S-22100, Lund, Sweden

Received December 16, 1999. Revised Manuscript Received March 20, 2000

Abstract: The low-lying electronic states of the *p*-benzosemiquinone radical anion are studied using multiconfigurational second-order perturbation theory (CASPT2) and extended atomic natural orbital (ANO) basis sets. Vertical excitation energies at the optimized geometries of the anion and the neutral molecule are computed. In light of the present theoretical results, the information provided by different spectroscopic techniques, such as UV/vis absorption, excitation, fluorescence, electron photodetachment, and electron scattering, is rationalized. CASSCF force fields are employed to compute vibronic intensities of the two lowest-energy $\pi-\pi^*$ transitions in order to solve controversial assignments and to give an interpretation of the available resonance Raman data.

1. Introduction

Quinone derivatives act as final electron acceptors in crucial biological processes such as photosynthesis and respiration.[1] The anionic electronic excited states of the chromophore, *p*-benzoquinone (PBQ), form a dense ladder of states which play an important role as intermediate steps in electron-transfer processes and enhance electron acceptor dynamics in natural systems.[2] A better understanding of the phenomena requires a detailed knowledge of the nature and properties of the *p*-benzosemiquinone radical anion (PBQ^-) low-lying excited states.

The complete active space (CAS)SCF approximation[3] in combination with a second-order perturbation approach, the CASPT2 method[4−6] has been shown to provide reliable predictions and interpretations of the electronic spectra of organic molecules in numerous applications.[7−9] In particular, a recent study of the electronic excited states of PBQ led to a full understanding of its electronic spectrum.[10] The analysis of the electronic structure of negative ions by using the CASPT2 method was successfully performed by Rubio et al. in a study of the spectrum of the biphenyl radical anion.[11] The ground and excited states of this system represent temporary anion states, which means that they are higher in energy than the ground state of the neutral system, that is, they are unstable with respect to electron detachment. Conventional quantum chemical techniques cannot be applied in general to the study of these temporary states, since they lie in the continuum of the neutral species plus the free electron.[12] Nevertheless, Rubio et al.[11] showed that, at the CASSCF level, it was possible to obtain well-localized solutions, which can be regarded as a discrete representation of the temporary anion states. Additional test calculations, in which the nuclear charges were slightly increased and the anion was computed in a solvent, confirmed the stable nature of the CASSCF solutions. The low-lying excited states of the biphenyl radical anion were thus calculated by using the CASSCF/CASPT2 procedure together with a basis set of atomic natural orbital (ANO) type, which included diffuse functions placed at the center of the molecule. The results obtained correlated well with the available spectroscopic data and allowed an interpretation of the experimental findings.

In the present contribution, the same theoretical approach has been chosen for carrying out an in-depth investigation of the low-lying electronic states of PBQ^-. Despite the relevance of quinone/semiquinone pairs for a wealth of important biological redox reactions and the large amount of information about the electronic structure of PBQ^- currently available, the character

(1) Stryer, L. *Biochemistry*; W. H. Freeman & Co., New York, 1995.
(2) Schiedt, J.; Weinkauf, R. *J. Chem. Phys.* **1999**, *110*, 304.
(3) Roos, B. O. The complete active space self-consistent field method and its applications in electronic structure calculations. In *Advances in Chemical Physics; Ab Initio Methods in Quantum Chemistry - II*; Lawley, K. P., Ed.; John Wiley & Sons Ltd., Chichester, England, 1987; Chapter 69, p 399.
(4) Andersson, K.; P.-Å. Malmqvist, Roos, B. O.; Sadlej, A. J.; Wolinski, K. *J. Phys. Chem.* **1990**, *94*, 5483.
(5) Andersson, K.; P.-Å. Malmqvist, and B. O. Roos. *J. Chem. Phys.* **1992**, *96*, 1218.
(6) Andersson, K.; Roos, B. O. Multiconfigurational second-order perturbation theory. In *Modern electron structure theory, Advanced Series in Physical Chemistry*; Yarkony, R., Ed.; World Scientific Publishing Co. Pte. Ltd.: Singapore, 1995; Vol. 2, Part I, p 55.
(7) Roos, B. O.; Fülscher, M. P.; Malmqvist, P.-Å.; Merchán, M.; Serrano-Andrés, L. Theoretical studies of electronic spectra of organic molecules. In *Quantum Mechanical Electronic Structure Calculations with Chemical Accuracy*; Langhoff, S. R.; Ed.; Kluwer Academic Publishers: Dordrecht, The Netherlands, 1995; p 357.
(8) Roos, B. O.; Andersson, K.; Fülscher, M. P.; Malmqvist, P.-Å.; Serrano-Andrés, L.; Pierloot, K.; Merchán, M. Multiconfigurational perturbation theory: Applications in electronic spectroscopy. In *Advances in Chemical Physics: New Methods in Computational Quantum Mechanics*; Prigogine, I., Rice, S. A., Eds.; John Wiley & Sons: New York, 1996; Vol. XCIII, p 219.
(9) Merchán, M.; Serrano-Andrés, L.; Fülscher, M. P.; Roos, B. O. Multiconfigurational perturbation theory applied to excited states of organic compounds. In *Recent Advances in Multireference Theory*; Hirao, K., Ed.; World Scientific Publishing: Singapore, 1999; Vol. IV, p 161.
(10) Pou-Amérigo, R.; Merchán, M.; Ortí, E. *J. Chem. Phys.* **1999**, *110*, 9536.
(11) Rubio, M.; Merchán, M.; Ortí, E.; Roos, B. O. *J. Phys. Chem.* **1995**, *99*, 14980.
(12) Simons, J.; Jordan, K. D. *Chem. Rev.* **1987**, *87*, 535.

10.1021/ja994402m CCC: $19.00
Published on Web 06/09/2000

and position of the excited states of this radical anion have not been fully clarified. Two major open questions about the spectroscopic behavior of the system are under debate. Is the vibrational structure of an electronic transition responsible for the two lowest-energy intense peaks detected in the electronic spectrum or are two close-lying electronic states involved? As shall be discussed below, the computation of vibronic frequencies and intensities is required to answer unambiguously this question. On the other hand, should the resonances detected in electron-scattering studies be attributed to the same electronic states that are responsible for the absorptions in the UV/vis spectrum? The calculation of the excited states of the anion at the geometry of the neutral system will give additional insights into this problem, and new assignments will be proposed. The correct interpretation of the available spectroscopic data is of crucial importance for the understanding of fundamental charge-transfer processes involving quinones, like ubiquinone and plastoquinone, which take place in living organisms.

2. Methods and Computational Details

The ground-state geometry of PBQ^- has been optimized at the CASSCF level by including the π and π^* valence molecular orbitals (eight MOs and nine electrons) in the active space (π-CASSCF). For sake of comparison, the same basis set employed in the previous study on the molecular structure of PBQ[10] has been used. It is an ANO type basis set contracted according to the scheme C,O[4s3p1d]/H[2s1p].[13] Calculations have been carried out within D_{2h} symmetry, with the molecule placed in the *yz* plane and the two oxygen atoms along the *z* axis. As far as we know, no geometrical experimental data are available. Nevertheless, the geometry of PBQ^- has been optimized employing very different approaches in numerous theoretical studies.[14−24] A D_{2h} lowest-energy structure has been always obtained for the ground state of the isolated radical anion.

For the computation of the vertical excitation energies, the same basis set previously used for the study of the electronic spectrum of the neutral molecule has been employed. It consists of the ANO basis set described above supplemented with a set of 1s1p1d diffuse functions placed at the center of the molecule.[10] The electronic states have been calculated by means of the CASPT2 approach.[4−6] In this method, the first-order wave function and the second-order energy are calculated using the CASSCF wave function as reference. Two active spaces were employed in the study. The π valence active space, which comprises eight active orbitals and nine electrons, was used for the calculation of the $\pi \rightarrow \pi^*$ transitions. Following the notation previously introduced,[10] it will be denoted by (9/03010301), where the first label gives the number of active electrons and the following labels indicate the number of active orbitals in each of the eight irreducible representations (a_g, b_{3u}, b_{2u}, b_{1g}, b_{1u}, b_{2g}, b_{3g}, and a_u) of the D_{2h} symmetry point group. For those transitions which show predominantly an $n \rightarrow \pi^*$ character, the two n valence orbitals were added to the active space. Thus, it will be denoted by (13/03110311). Extra orbitals had to be included in the active space for the computation of the $^2B_{3g}$ and $^2B_{3u}$ states, to minimize the effect of intruder states in the CASPT2 treatment. In the case of the $^2B_{3g}$ state, the active space was enlarged to (15/03110321) by including the $3b_{3g}$ orbital, and the $4b_{3u}$ one-electron function was added in the calculation of the $\pi\pi^*$ $^2B_{3u}$ excited states, computed with the active space (9/04010301). All excitations energies have been obtained using the ground-state energy computed with the same active space used in the calculation of the corresponding excited state. The carbon and oxygen 1s electrons were kept frozen in the form determined by the SCF wave function, and they were not included in the second-order correlation treatment. The CASSCF state interaction (CASSI) method[25,26] has been employed to compute the transition dipole moments. Energy differences corrected by CASPT2 correlation energies have been used in the oscillator strength formula.

Adiabatic electron affinities were estimated by calculating the ground-state energy difference between the neutral molecule and the anion at the corresponding CASSCF optimized geometries. The basis sets and procedures chosen for the computation of this property have been identical to those employed in the study of the vertical excited states. Besides the discrete valence temporary anion states, diffuse states described by a singly excited configuration involving a diffuse orbital were also obtained in some cases. These solutions try to simulate the neutral molecule plus a free electron by putting the extra electron into the most diffuse orbital available. Thus, the computed energy for these states strongly depends on the diffuseness of the basis set employed. Therefore, the so-computed unstable solutions have not been further considered.

A somewhat larger ANO-type basis set, with the contraction scheme C,O[4s3p2d]/H[3s2p],[13] which has been shown to lead to accurate force fields for benzene,[27] has been used for the vibrational studies. The π-valence active space has been employed to obtain, at the CASSCF level, the optimized geometries and analytical second derivatives of the energy with respect to the nuclear coordinates needed for the vibrational analysis of the three studied states: 1^2B_{2g}, 1^2B_{3u}, and 1^2A_u. The matrix elements describing the transition moment function are expressed in terms of Franck−Condon factors, that is, overlaps between two sets of harmonic oscillator functions representing the force fields of the participating states. As the transitions from the ground state of PBQ^- to the two studied excited states are one-photon dipole allowed, it is possible to focus the analysis of the vibronic transition moment on the zeroth-order term of the Herzberg−Teller expansion, that is, within the Condon approximation, and discard the contributions from high-order terms. Calibration calculations demonstrated that the intensity obtained from high-order terms is not relevant for the present analysis. The finally computed parameter is the oscillator strength of the transition, obtained as:

$$f = \frac{2}{3}\Delta E\, M^2_{gi,fj} \tag{1}$$

where ΔE is the transition energy and $M^2_{gi,fj}$ the vibronic transition moment, computed as:

$$M_{gi,fj} = M_{gf}(Q_0)\,\langle \phi_i(Q) \mid \phi_j(Q)\rangle \tag{2}$$

where *gi* and *fj* are the initial and final vibronic states, respectively and $\phi(Q)$ represent the vibrational functions. $M_{gf}(Q_0)$ is the electronic transition dipole moment function, evaluated at the initial state geometry by means of the CAS state-interaction (CASSI) method.[25,26] The vibrational wave functions use force fields taken directly from the second derivatives, with no adjustment for anharmonicities. A full explanation of the procedure followed to obtain the vibronic intensities can be found in ref 27. While geometries, force fields, and electronic transition dipole moments have been calculated at the CASSCF level, the band origins (0−0 transitions) have been obtained by computing CASPT2 energies at the CASSCF geometry minima of the corresponding states (including the zero-point vibrational correction). The Herzberg

(13) Widmark, P.-O.; Malmqvist, P.-Å.; Roos, B. O. *Theor. Chim. Acta*, **1990**, *77*, 291.
(14) Chipman, D. M.; Prebenda, M. F. *J. Phys. Chem.* **1986**, *90*, 5557.
(15) Wheeler, R. A. *J. Phys. Chem.* **1993**, *97*, 1533.
(16) Raymond, K. S.; Wheeler, R. A. *J. Chem. Soc., Faraday Trans. 2* **1993**, *89*, 665.
(17) Liu, R.; Zhou, X. *J. Phys. Chem.* **1993**, *97*, 9613.
(18) Nonella, M. *J. Phys. Chem. B* **1997**, *101*, 1235.
(19) Mariam, Y. H.; Chantranupong, L. *J. Comput.-Aided Mol. Des.* **1997**, *11*, 345.
(20) Mohandas, P.; Umapathy, S. *J. Phys. Chem. A* **1997**, *101*, 4449.
(21) Boesch, S. E.; Wheeler, R. A. *J. Phys. Chem. A* **1997**, *101*, 8351.
(22) Eriksson, L. A. Himo, F.; Siegbahn, P. E. M.; Babcock, G. T. *J. Phys. Chem. A* **1997**, *101*, 9496.
(23) Zhan, C.-G.; Iwata, S. *Chem. Phys.* **1998,** *230*, 45.
(24) Zhan, C.-G.; Chipman, D. M. *J. Phys. Chem. A* **1998**, *102*, 1230.
(25) Malmqvist, P.-Å. *Int. J. Quantum Chem.* **1986**, *30*, 479.
(26) Malmqvist, P.-Å.; Roos, B. O. *Chem. Phys. Lett.* **1989**, *155*, 189.
(27) Bernhardsson, A. Forsberg, N.; Malmqvist, P.-Å.; Roos, B. O.; Serrano-Andrés. L. *J. Chem. Phys.* **2000**, *112*, 2798.

Table 1. Geometrical Parameters for the Ground States of *p*-Benzoquinone (PBQ), 1^1A_g, and *p*-Benzosemiquinone Radical Anion (PBQ^-), 1^2B_{2g}, Optimized at the π-CASSCF Level,[a] and Adiabatic Electron Affinity (EA) of *p*-Benzoquinone

parameter[b]	PBQ	PBQ^-
r(C═O)	1.210	1.246
r(C═C)	1.343	1.369
r(C−C)	1.479	1.443
r(C−H)	1.074	1.078
∠(C−C_O−C)	117.4	114.7
∠(C═C−H)	122.2	120.4
EA (CASSCF) = −0.33 eV		
EA (CASPT2) = 2.01 eV		
EA (exp) = 1.91± 0.06 eV[c], 1.860 ± 0.005 eV[d]		

[a] ANO C,O[4s3p1d]/H[2s1p] basis set. [b] Bond distances in Å and angles in degrees. C_O denotes a carbon atom bound to an oxygen atom. [c] Determined from gas-phase electron-transfer equilibria measurements, refs 54,55. [d] Determined from resonant photodetachment photoelectron spectra, ref 2.

convention[28] of numbering the normal modes has been employed throughout. The vibrational spectra computed in the present study were convoluted with a Lorentzian function of full width at half-maximum $\Gamma = h/(4\pi T_2)$ corresponding to a fictitious lifetime $T_2 = 130$ fs to account for the finite experimental resolution and for degrees of freedom not considered here, such as rotation. The effect of the temperature has been considered by including a population of the vibrational states through a Boltzmann distribution at 300 K.

All calculations have been performed with the MOLCAS-4 program package.[29]

3. Results and Discussion

3.1. Geometry and Electron Affinity. The equilibrium geometrical parameters computed at the π −CASSCF level for the ground state of PBQ^-, 1^2B_{2g}, together with those obtained for the ground state of the neutral molecule, 1^1A_g, at the same level of calculation,[10] are collected in Table 1.

Addition of an electron to PBQ yields significant changes in the structural parameters. The C═O and C═C bonds are elongated by 0.036 and 0.026 Å, respectively, whereas the C−C bonds are shortened by 0.036 Å. These modifications reveal that the quinonoid character of the neutral molecule is partially lost upon reduction. The ring becomes more benzenoid, with smaller differences between the single and double carbon−carbon bonds, and the carbon−oxygen bond length increases. The changes can be rationalized on the basis of a simple MO model. The ground state of the radical anion is mainly described by a configuration which can be built by considering the principal configuration of the ground state of the neutral molecule and adding the extra electron to the lowest unoccupied MO (LUMO). The LUMO belongs to the b_{2g} symmetry and exhibits bonding character over the C−C bonds and antibonding character over the C═C and C═O bonds. Consequently, the electron attachment is expected to shorten the single bonds and lengthen the double ones. Similar geometrical changes were also obtained in recent theoretical treatments.[18,20−23] These changes are consistent with those concerning the vibrational frequencies reported in a resonance Raman study.[30] The frequencies of the modes mainly involving C−C stretching increase upon reduction, while those involving C═O and C═C stretching decrease.

Table 2. Computed Vertical Excitation Energies and Oscillator Strengths for the Electronic States of the *p*-Benzosemiquinone Radical Anion; Experimental Data Are also Included

state	excitation energies (eV) CASSCF	CASPT2	exp[a]	osc. str.[b]
Ground State: 1^2B_{2g}				
1^2B_{2u}	2.92	2.23	2.27[c]	forbidden
1^2B_{3g}	2.88	2.25	2.41[c]	forbidden
1^2B_{3u}	3.83	2.80	2.77(2.94)[d]	0.0532(0.15,0.06)
1^2A_u	2.89	2.82	∼3.26[e]	0.1044(0.17,0.03)
1^2B_{1g}	3.60	3.25		forbidden
2^2B_{3u}	5.26	3.56	3.84(3.91)[f]	0.3203(0.50,0.35)

[a] Absorption maxima in acetonitrile taken from ref 30, unless otherwise stated. Additional absorptions attributed to the vibrational structure within parentheses. [b] Experimental values (in ethanol, in water) within parentheses. Taken from refs 33,35, respectively. [c] Position of the resonances in the photodetachment spectrum, ref 2. [d] The position of the main peak ranges from 2.73 to 2.92 eV (vibrational peak from 2.94 to 3.08 eV) depending on the solvent, refs 30, 33, 35−38, 40, 42, 56. The lowest-energy values correspond to less polar solvents. [e] Shoulder detected between 3.22 and 3.40 eV, depending on the solvent, refs 30, 33, 35, 36, 42. The lowest-energy values correspond to less polar solvents. [f] The position of the main peak ranges from 3.80 to 3.94 eV (vibrational peak from 3.91 to 4.03 eV) depending on the solvent, refs 30, 33, 35−37. The lowest-energy values correspond to less polar solvents.

The adiabatic electron affinity of PBQ computed at different levels of theory is shown in Table 1. Experimental data are also included in Table 1 for comparison. The measured electron affinity is positive and rather high, consistent with the well-known ability of PBQ to act as electron acceptor both in charge-transfer complexes and in biological redox reactions. Incidentally, the ground state of the anion is predicted to lie above the ground state of the neutral molecule at the CASSCF level, and therefore, a negative adiabatic electron affinity is obtained. Addition of the dynamic correlation energy corrects such a wrong behavior and leads to the computed value of 2.01 eV, in agreement with the available experimental data (cf. Table 1). This significant change reflects the importance of a balanced treatment of the different correlation energy effects for the accurate computation of the electron affinity, which is, for this reason, a usually difficult property to be determined accurately on theoretical grounds.

3.2. Vertical Excited States. 3.2.1. Spectrum Region: 2.2−2.5 eV. The results obtained at the CASSCF/CASPT2 level for the electronic states of PBQ^- are collected in Table 2, together with the available experimental data. The optimized geometry of the radical anion, listed in Table 1, has been employed for these calculations. Figure 1 contains the most important electronic configurations and their weights in the CASSCF wave functions describing the ground and excited states of PBQ^-. For the sake of clarity, the same notation that was used in the previous study of PBQ[10] will be employed. Therefore, terms such as HOMO (H) or LUMO (L) refer to the corresponding orbitals in the neutral molecule.

The ground state of PBQ^- belongs to the $^2B_{2g}$ symmetry. The wave function is dominated by a single configuration with the following occupation: $(1b_{3u})^2\,(1b_{2g})^2\,(5b_{2u})^2\,(4b_{3g})^2\,(2b_{3u})^2\,(1b_{1g})^2\,(2b_{2g})^1$. It corresponds to the principal configuration of the ground state of PBQ and the extra electron placed in the $2b_{2g}$ π^*-orbital, that is, the LUMO.

The lowest-lying doublet excited states of the ion are predicted to be the 1^2B_{2u} and the 1^2B_{3g} electronic states. At the CASPT2 level, they are located between 2.2 and 2.3 eV above

(28) Herzberg, G. *Molecular Spectra and Molecular Structure III*; *Electronic Spectra and Electronic Structure of Polyatomic Molecules*; Van Nostrand: New York, 1966.

(29) Andersson, K. Blomberg, M. R. A.; Fülscher, M. P.; Karlström, G.; Lindh, R.; Malmqvist, P.-Å.; Neogrády, P.; Olsen, J.; Roos, B. O.; Sadlej, A. J.; Schütz, M.; Seijo, L.; Serrano-Andrés, L.; Siegbahn, P. E. M.; Widmark, P.-O. *MOLCAS*, version 4.0; Department of Theoretical Chemistry, Chemical Center: University of Lund, Sweden, 1997.

(30) Zhao, X.; Imahori, H.; Zhan, C.-G.; Sakata, Y.; Iwata, S.; Kitagawa, T. *J. Phys. Chem. A* **1997**, *101*, 622.

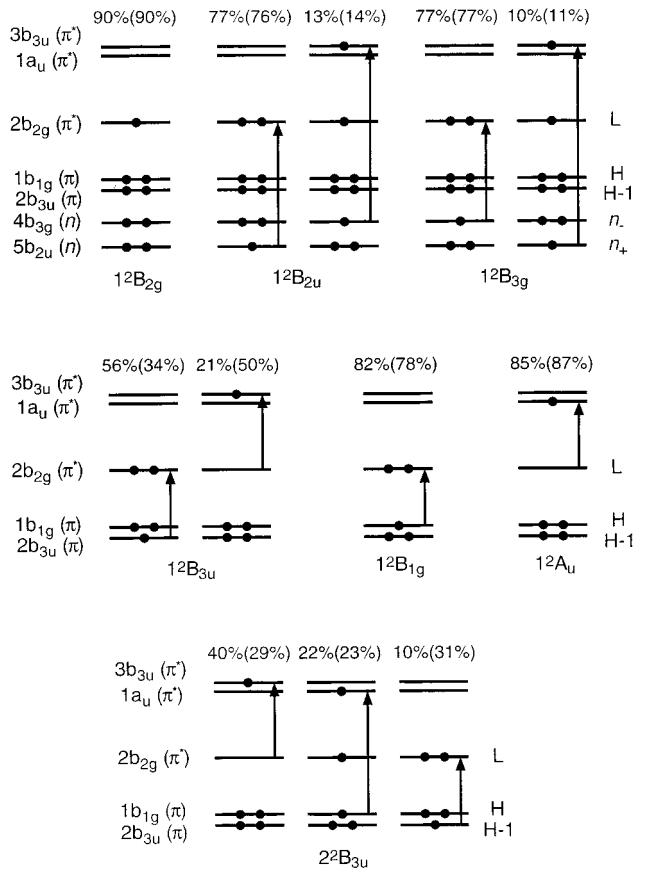

Figure 1. The most important electronic configurations in the CASSCF wave function for the low-lying states of the *p*-benzosemiquinone radical anion. The orbital occupation and the weight in the wave function are given. The weights obtained at the optimized geometry of neutral *p*-benzoquinone are indicated within parentheses.

the ground state of the radical anion. The transitions $1^2B_{2g} \rightarrow 1^2B_{2u}$ and $1^2B_{2g} \rightarrow 1^2B_{3g}$ are dipole forbidden. Taking as reference the main configuration of the $^2B_{2g}$ ground state, the CASSCF wave functions of these excited states are dominated by n → L one-electron excitations, that is, the promotion of an electron from a doubly occupied n orbital to the half occupied π^* LUMO, closing the LUMO shell (see Figure 1). It is worth mentioning that, at the optimized geometry of the anion, the vertical detachment energy is computed to be 2.10 eV at the CASPT2 level. The lowest-lying excited states lie, therefore, slightly above the detachment threshold. Consequently, these states, as well as the higher-lying excited states, represent temporary negative ion states, the so-called resonances, which will be unstable with respect to the ground state of the neutral molecule and a free electron. The metastable states of anions can be classified as either shape or core-excited resonances (see, e.g., ref 12 and references therein). From the electronic structure standpoint, shape resonances originate in the attachment of the electron to a virtual orbital. Alternatively, they can be viewed as the result of the promotion of the unpaired electron of the LUMO to higher-lying virtual orbitals. Core-excited resonances can be seen, however, as arising from the attachment of an extra electron to an excited state of the neutral molecule. They can be divided into Feshbach and core-excited shape resonances, depending on their energetic position with respect to excited state of the neutral molecule involved. The former lie below the parent state of the neutral, whereas the latter are located above. In the case of the 1^2B_{2u} and the 1^2B_{3g} states of PBQ^-, their main configurations can be interpreted as the attachment of the surplus electron to the LUMO of PBQ in its n → L excited states. Therefore, they represent core-excited resonances. The n → L states of the neutral molecule (1^1B_{1g} and 1^1A_u) were also computed to be the lowest-lying excited states.[10] They were predicted to be degenerate at the CASPT2 level, with an excitation energy of 2.50 eV with respect to the ground state of the neutral molecule. Thus, the resonances lie below the corresponding excited states of the neutral molecule, and therefore, they can be labeled as Feshbach resonances.

Even though the occurrence of these low-lying excited states was early predicted by theoretical calculations,[31] this region of the spectrum has not received much attention from the experimental point of view. The most complete information has been obtained recently from the excitation and fluorescence spectra reported by Cook et. al.[32] and from the photodetachment spectra measured by Schiedt and Weinkauf.[2]

In the excitation spectrum of PBQ^- in a rigid matrix, Cook et al. observed a weak tail in the energy range 2.25−2.5 eV.[32] The authors proposed that this feature might represent an absorption band with an origin near 2.1 eV, corresponding to a forbidden transition which borrows intensity from the strong band located around 2.7−2.8 eV. The fluorescence spectrum after optical excitation at 2.71 eV produced an emission with an apparent origin at 2.09 eV and an initial peak at 2.04 eV. These values agree with those estimated from the excitation spectrum. They concluded that the emission and the strong absorption bands did not arise from the same state. A mechanism was instead suggested in which the process starts with an intense absorption around 2.7−2.8 eV, involving a higher-energy state, followed by a rapid internal conversion to the final fluorescent state.

Schiedt and Weinkauf analyzed the photodetachment spectrum of PBQ^- at energies slightly above the photodetachment threshold.[2] In the photon energy range of 2.20−2.45 eV, they found six sharp peaks. The three lowest-energy features (located at 2.21, 2.23, and 2.27 eV) were attributed to a first state and the three remaining peaks (placed at 2.40, 2.41, and 2.43 eV) to a second state. The energetic spacing within each group was adscribed to vibrational effects. On the basis of the spectral behavior, the recorded features were assigned to two Feshbach resonances.

The theoretical results obtained at the CASPT2 level confirm the assignments proposed by Schiedt and Weinkauf, providing an interpretation of the experimental data. Two forbidden transitions are computed to be the lowest-energy excitations, $1^2B_{2g} \rightarrow 1^2B_{2u}$ and $1^2B_{2g} \rightarrow 1^2B_{3g}$, which are found to lie in the same energy range where the weak tail in the excitation spectrum is detected. Moreover, the absorption around 2.7−2.8 eV does not lead to these low-energy nπ^* states, but to an allowed $\pi\pi^*$ higher-energy state (cf. Table 2). The theoretical findings give support to the suggestion offered by Cook et al.[32] concerning the nature and position of the states responsible for the intense absorption and for the weak fluorescence. The theoretical prediction of only two electronic states between 2.20 and 2.45 eV also supports the assignment of the six sharp peaks of the photodetachment spectrum to two different states proposed by Schiedt and Weinkauf[2], even though the calculated separation between the states (0.02 eV) is smaller than that obtained between the maxima of the two groups of peaks (0.14 eV). According to the theoretical results, these states correspond to Feshbach resonances, in agreement with the experimental

(31) Chang, H. M.; Jaffé, H. H.; Masmanidis, C. A. *J. Phys. Chem.* **1975**, *79*, 1118.

(32) Cook, A. R.; Curtiss, L. A.; Miller, J. R. *J. Am. Chem. Soc.* **1997**, *119*, 5729.

conclusions.[2] This successful rationalization of the photodetachment spectrum could be, however, fortuitous. It should be pointed out that the relative positions of the $^2B_{2u}$ and $^2B_{3g}$ states with respect to the ground state of the neutral molecule and, therefore, the Feshbach resonance character of these states cannot be unambiguously established at present. The involved states are within 0.15 eV, the error bar of the method. Moreover, small modifications of the optimized geometric parameters might yield a different ordering of the electronic states and, consequently, a change in their nature.

From a theoretical point of view, the existence of two lowest-lying excited states of $^2B_{2u}$ and $^2B_{3g}$ symmetries has been also predicted by several authors, using both semiempirical[31,32] and ab initio[2,15,32] approaches. Even though the ordering of the states is different depending on the method, the computed excitation energies do not deviate very much from the experimental values, except those obtained with the SCF-CI procedure, which are overestimated by 0.8−1.0 eV.[15] The remaining ab initio values previously reported show deviations smaller than 0.35 eV, either overestimations (at the CASSCF level[15]) or underestimations (at the MP2 level[32]). Schiedt and Weinkauf have recently reported some unpublished results obtained by Sobolevski and Domcke at the CASPT2 level of calculation.[2] The excitation energies of the $^2B_{2u}$ and $^2B_{3g}$ states were computed to be 2.26 and 2.37 eV, respectively. These values were, indeed, used by Schiedt and Weinkauf for the assignment of the six sharp peaks to both states. The relative position of the two states was identical to that obtained here, but the separation between them was larger.

3.2.2. Spectrum Region: 2.5−4.2 eV. The scarce experimental information concerning the lowest-lying excited states of PBQ^- strongly contrasts with the numerous studies of the states placed in the energy interval 2.5−4.2 eV. The UV/vis absorption spectra of PBQ^- in different solvents exhibit, in this region, the most intense bands. They consist of two closely spaced peaks between 2.7 and 3.1 eV, a very broad band around 3.3 eV, and a very intense band in the region 3.8−4.2 eV.[30,33−37] The latter presents the largest oscillator strength.[33,35] However, for the other peaks the values reported do not allow to reach a definitive conclusion about their relative intensities. The accurate determination of the position of the broadest 3.3-eV band has been a difficult task. In some cases, it is described just as a shoulder[35] or as an unresolved shoulder.[38,39] In other cases, only an approximate location is given.[30,36]

The first clues for the interpretation of these absorption bands were provided by Harada and Inokuchi.[40,41] They recorded the electronic spectrum of several *p*-benzosemiquinone radical anions. Even though they were not able to observe all these features in the case of the non-substituted anion, they found them in several derivatives. On the basis of the magnitude of the intensities, they proposed that $\pi-\pi^*$ allowed transitions were responsible for these absorption bands. In addition, the two lowest-energy absorption maxima, located at 2.87 and 3.04 eV, were considered to be caused by the same electronic transition and the splitting ($\sim$1400 cm^{-1}) was attributed to the C−O stretching frequency in the excited state.[40] These hypotheses were supported by the results of semiempirical calculations on the non-substituted anion,[41] which predicted only three allowed electronic states in this region of the spectrum. The states exhibited $\pi-\pi^*$ character and were of B_{3u}, A_u, and B_{3u} symmetries. The ground state was predicted to be a $^2B_{2g}$ state. The experimental determination of all these absorption bands for the non-substituted PBQ^- was achieved in further studies[33−35]. According to the classification by Harada et al., the features were distributed into three bands, which were attributed to $^2B_{2g} \rightarrow {}^2B_{3u}$, $^2B_{2g} \rightarrow {}^2A_u$, and $^2B_{2g} \rightarrow {}^2B_{3u}$ transitions, in increasing order of energy. On the other hand, Chang et al.,[31] on the basis of semiempirical CNDO/S calculations, proposed a different assignment where the 1^2B_{3u} and 1^2A_u states ordering was reverted in order to match the intensity patterns.

Resonance Raman studies[30,36,38,39,42,43] have given important insights into the nature of the excited electronic states of PBQ^-. The Raman spectra obtained by excitation in resonance with the lowest-energy intense absorption showed the strongest enhancement for the vibrational band located at 1620 cm^{-1}.[36,38,39,43] This frequency was attributed to the ν_2 mode (Herzberg's notation), which primarily involves in-phase expansion of the double C−C bonds and in-phase contraction of the single C−C bonds.[38,39] As it is well-known, the greatest enhancements in the bands of the Raman spectrum correspond to those vibrational modes which are most responsible for the changes in the equilibrium geometry in passing from the ground to the corresponding excited state, since the Franck−Condon overlaps are, in these cases, large. Tripathi and Schuler[39] estimated the geometric changes associated to the electronic transitions by means of a semiempirical evaluation of the bond orders in the different states. Similar changes to those involved in ν_2 were found for the $1^2B_{2g} \rightarrow 1^2B_{3u}$ excitation, whereas the $1^2B_{2g} \rightarrow 1^2A_u$ transition was predicted to cause an expansion of all the carbon−carbon bonds. The former was, therefore, assigned as responsible for the lowest-energy intense band of the spectrum. The ν_2 vibrational mode was expected to form progression in the electronic absorption spectrum. Consequently, the splitting between the two peaks in the 2.7−3.1 eV region was attributed to this C−C stretching frequency in the excited state. This conclusion disagreed with that proposed by Harada and Inokuchi, who suggested a C−O stretching frequency.[40] The broad band around 3.3 eV was assigned to the $^2B_{2g} \rightarrow {}^2A_u$ transition.[36,39] The Raman spectrum of PBQ^- excited in resonance with this band showed an enhancement of the ring breathing mode,[36] which was consistent with the estimated geometric changes of the transition to the ^2A_u state.[39] Moreover, two vibrational modes of b_{3g} symmetry were also enhanced.[36] They could gain intensity through vibronic coupling with a nearby intense electronic transition such as that observed at 3.8−4.2 eV.[36] The requirements of symmetry impose this transition to be $^2B_{2g} \rightarrow {}^2B_{3u}$. In a recent study of the resonance Raman spectra of PBQ^- obtained by exciting in resonance with the three lowest-energy intense bands, identical assignments have been proposed.[30]

Recent theoretical studies give different interpretations for the intense bands depending on the approach. On one hand, SCF−CI and CASSCF calculations[15] obtained the state ordering $^2B_{3u}$, ^2A_u, and $^2B_{3u}$. Nevertheless, the excitation energies showed, in some cases, large deviations with respect to the experimental values. On the other hand, MP2 as well as semiempirical

(33) Kimura, K.; Yoshinaga, K.; Tsubomura, H. *J. Phys. Chem.* **1967**, *71*, 4485.
(34) Kimura, K.; Yamada, H.; Tsubomura, H. *J. Chem. Phys.* **1968**, *48*, 440.
(35) Fukuzumi, S.; Ono, Y.; Keii, T. *Bull. Chem. Soc. Jpn.* **1973**, *46*, 3353.
(36) Tripathi, G. N. R.; Schuler, R. H. *Chem. Phys. Lett.* **1989**, *156*, 51.
(37) Zhao, X.; Kitagawa, T. *J. Raman Spectrosc.* **1998**, *29*, 773.
(38) Tripathi, G. N. R. *J. Chem. Phys.* **1981**, *74*, 6044.
(39) Tripathi, G. N. R.; Schuler, R. H. *J. Chem. Phys.* **1982**, *76*, 2139.
(40) Harada, Y.; Inokuchi, H. *Mol. Phys.* **1964**, *8*, 265.
(41) Harada, Y. *Mol. Phys.* **1964**, *8*, 273.
(42) Hester, R. E.; Williams, K. P. J. *J. Chem. Soc., Faraday Trans. 2* **1982**, *78*, 573.
(43) Schuler, R. H.; Tripathi, G. N. R.; Prebenda, M. F.; Chipman, D. M. *J. Phys. Chem.* **1983**, *87*, 5357.

calculations yielded $1^2B_{2g} \rightarrow 1^2A_u$ as the lowest-energy allowed transition.[32] Furthermore, unpublished CASPT2 calculations placed the lowest-energy $\pi\pi^*$ transition ($1^2B_{2g} \rightarrow 1^2A_u$) at 2.78 eV.[2] On the basis of this result, the broad peak at 2.50 eV found in the photodetachment spectrum of PBQ^-, attributed to the origin of a shape resonance, was assigned to the ^2A_u state.[2] Therefore, the band assignment is still an open question.

As can be seen in Table 2, the CASSCF/CASPT2 calculations carried out in the present work place four electronic states in the energy range 2.5−4.2 eV. They are the 1^2B_{3u} and 1^2A_u states, with excitation energies around 2.8 eV and computed to lie very close in energy, the 1^2B_{1g} state, located at 3.25 eV, and the 2^2B_{3u} state, placed 3.56 eV above the ground state. Transition to the B_{1g} state is dipole forbidden, whereas the remaining are dipole allowed. The most important configurations of the corresponding CASSCF wave functions, depicted in Figure 1, involve promotions implying only π orbitals. The B_{3u} states have significant multiconfigurational character. Three basic configurations are involved: H-1 → L, L → $3b_{3u}$, and H → $1a_u$. The 1^2B_{3u} is mainly described by the two first configurations (56 and 21%, respectively) and the 2^2B_{3u} state by the second and the third configurations (40 and 22%, respectively). The ^2A_u and $^2B_{1g}$ states are essentially singly excited configurations, a shape resonance (L → $1a_u$) and a core-excited resonance (H → L), respectively. The latter is computed to lie 3.25 eV above the ground state of the radical anion, whereas the corresponding excited state of the neutral molecule (1^1B_{3g}) was found 4.19 eV above the ground state of PBQ.[10] Consequently, the negative ion state corresponds to a Feshbach resonance. The oscillator strengths for the $1^2B_{2g} \rightarrow 1^2B_{3u}$, $1^2B_{2g} \rightarrow 1^2A_u$, and $1^2B_{2g} \rightarrow 2^2B_{3u}$ allowed transitions are computed to be 0.0532, 0.1044, and 0.3203, respectively.

To check that these states were the only candidates for the assignment of the optical absorption bands in this region, additional calculations were carried out. First, higher-lying $n\pi^*$ and $\pi\pi^*$ excited states were computed. The excitation energies obtained confirmed that these states were placed more than 1 eV above the 2^2B_{3u} state. They were not located in the energy range considered and, therefore, they can be excluded. Second, electronic states which represent excitations of the unpaired electron to a valence σ^* orbital (L → σ^*) were also analyzed. One σ^* orbital of specific symmetry (a_g, b_{2u}, b_{1u}, or b_{3g}) was added to the active space to compute four new excited states. Therefore, $9e^-$ /9MOs active spaces were employed. The $^2B_{3g}$ state was computed to lie in a higher-energy range, with a predicted excitation energy of 5.63 eV. Regarding the other three L → σ^* states, they were located between 3.7 and 4.1 eV above the ground state. Transitions to the ^2A_g and $^2B_{2u}$ are optically forbidden. Despite the dipole-allowed character of the transition to the $^2B_{1u}$ state, its oscillator strength was computed to be a hundred times smaller than that corresponding to the $1^2B_{2g} \rightarrow 2^2B_{3u}$ excitation. Therefore, the contribution of these states to the absorption spectrum can be confidently considered to be negligible.

The results obtained in the present work give important insights into the interpretation of the experimental data. The most intense band of the electronic spectrum has been detected around 3.8 eV. According to the CASPT2 findings, only the $1^2B_{2g} \rightarrow 2^2B_{3u}$ excitation can be responsible for that feature. It exhibits the largest oscillator strength and the excitation energy is computed to be 3.56 eV. This gives further support to the assignment proposed by Tripathi and Schuler,[36] confirming also previous theoretical predictions.[15,31,41] The assignment of the lower-energy features found in the 2.7−3.4 eV interval is, however, far from being evident. Two electronic states, 1^2B_{3u} and 1^2A_u, are predicted to be quasi-degenerate at the CASPT2 level, and are computed to lie in the same energy region where the two first intense peaks occur, that is, between 2.7 and 3.1 eV. These peaks have been adscribed to vibrational structure of the same absorption band. The assignment is even more difficult for the broad band located around 3.3 eV, since no allowed state is predicted in this region. The 1^2B_{1g} is computed to lie at 3.25 eV, but the transition from the ground state is forbidden.

Table 3. Geometrical Parameters for the 1^2B_{2g} (ground), 1^2B_{3u}, and 1^2A_u States of the *p*-Benzosemiquinone Radical Anion (PBQ^-) Optimized at the π-CASSCF Level within the D_{2h} Symmetry[a]

parameter[b]	1^2B_{2g}	1^2B_{3u}	1^2A_u
r(C═O)	1.244	1.301	1.227
r(C═C)	1.369	1.404	1.393
r(C−C)	1.443	1.418	1.466
r(C−H)	1.075	1.074	1.072
∠(C−C_O−C)[c]	114.8	116.5	119.6
∠(C═C−H)	120.4	120.0	123.0

[a] ANO C,O[4s3p2d]/H[3s2p] basis set. [b] Bond distances in Å and angles in degrees. [c] C_O denotes a carbon atom bound to an oxygen atom.

Although both the 1^2B_{3u} and the 1^2A_u states have been suggested as responsible for the lowest-energy intense band of the spectrum, the most conclusive experimental results assign the feature to the former, on the basis of resonance Raman data.[30,38,39] The 1^2B_{3u} state is also pointed out by the CASPT2 calculations as the most plausible candidate for such a feature, but the energy difference between the states is so small that any assignment would be only tentative and a definitive interpretation requires additional theoretical data. Likewise, it is not possible to elucidate whether the existence of two peaks is due to the vibrational structure or to the occurrence of two allowed electronic states close in energy.

With respect to the feature at 3.3 eV, it has been assigned to the $1^2B_{2g} \rightarrow 1^2A_u$ excitation on the basis of Raman measurements.[36,39] If we assume such an assignment, the CASPT2 excitation energies would deviate 0.4 eV from the experimental value. The error would be larger than expected for the method (with the employed basis set). Nevertheless, it is worth noting that the shape of the feature observed in the UV/vis spectra does not allow an accurate determination of its position. The absorption profile shows a shoulder, and it is difficult to locate the maximum and to evaluate the oscillator strength. Indeed, in some of the reported spectra, the shape of the shoulder suggests that the maximum might be placed at lower energies, but masked by the adjacent band, and that the feature observed might correspond to the tail of a broad band.

The full interpretation of the electronic spectrum can only be achieved by answering all of these open questions. The analysis of the vertical excitation energies does not provide, in this case, enough information to establish the nature of the observed bands. An additional study of the vibronic transitions is, therefore, necessary for the understanding of the spectrum in this energy region, as it is shown in the next section.

3.3. Vibrational Analysis of the $1^2B_{2g} \rightarrow 1^2B_{3u}$ and $1^2B_{2g} \rightarrow 1^2A_u$ Absorption Bands. A recent study of the vibronic frequencies and intensities of the low-lying absorption bands of the benzene molecule was successfully performed[27] and led to an accurate description of the main vibrational features. A similar study has been carried out here. Table 3 compiles the geometric parameters for the 1^2B_{2g}, 1^2B_{3u}, and 1^2A_u states of PBQ^- optimized at the π-CASSCF level using the ANO C,O[

Table 4. Harmonic Frequencies (ω_e, cm^{-1}) for the 1^2B_{2g} (ground), 1^2B_{3u}, and 1^2A_u States of the *p*-Benzosemiquinone Radical Anion (PBQ^-)

		theoretical[a]			experimental[b]	
sym	modes[c]	1^2B_{2g}	1^2B_{3u}	1^2A_u	1^2B_{2g}	1^2B_{2g}
a_g	ν_1 (ν_2)	3307	3317	3345		
	ν_2 (ν_{8a})	1798	1694	1737	1609	1620[e]
	ν_3 (ν_{7a})	1608	1296	1605	1452	1435[e]
	ν_4 (ν_{9a})	1239	1186	1202	1143	1161[e]
	ν_5 (ν_1)	864	877	834	819	
	ν_6 (ν_{6a})	499	492	482	470	481[e]
a_u	ν_7 (ν_{17a})	995	916	505		
	ν_8 (ν_{16a})	434	441	*i*351[d]		
b_{1g}	ν_9 (ν_{10a})	808	786	409	748	
b_{1u}	ν_{10}(ν_{20a})	3278	3294	3319		
	ν_{11}(ν_{12})	1688	1551	1727		
	ν_{12}(ν_{19a})	1486	1212	1461	1347	1504[f]
	ν_{13}(ν_{13})	1022	1055	1009		
	ν_{14}(ν_{18a})	850	827	816	780	
b_{2g}	ν_{15}(ν_5)	980	909	764		
	ν_{16}(ν_4)	803	719	686		
	ν_{17}(ν_{10b})	351	351	287		
b_{2u}	ν_{18}(ν_{20b})	3303	3311	3338		
	ν_{19}(ν_{19b})	1586	1382	1662	1506	1468[f]
	ν_{20}(ν_{15})	1198	1202	1453		
	ν_{21}(ν_{14})	1062	670	1103	1046	
	ν_{22}(ν_{18b})	407	375	458		
b_{3g}	ν_{23}(ν_{7b})	3279	3291	3314		
	ν_{24}(ν_{8b})	1583	1570	1426	1453	1472[e]
	ν_{25}(ν_3)	1366	1363	1146	1257	1271[e]
	ν_{26}(ν_{9b})	680	686	641	638	
	ν_{27}(ν_{6b})	506	456	462	497	
b_{3u}	ν_{28}(ν_{17b})	895	820	772		
	ν_{29}(ν_{16b})	555	533	544	525	
	ν_{30}(ν_{11})	144	157	130		

[a] π-CASSCF results within the D_{2h} symmetry. [b] Resonance Raman spectra in acetonitrile[30] unless specified. [c] Herzberg's convention[57] (Wilson's convention[58]). [d] Imaginary frequency found within the D_{2h} symmetry. [e] Resonance Raman spectra in water, refs 36 and 43. [f] Reference 59.

4s3p2d]/H[3s2p][13] basis set within the D_{2h} molecular symmetry. Deviations smaller than 0.003 Å in the distances and 0.1° in the angles are observed for the 1^2B_{2g} (ground) state geometry when compared to the data in Table 1 using a smaller basis set. Different effects are observed on the relaxed geometries upon excitation into the 1^2B_{3u} and 1^2A_u states. The former presents elongation of the double C−C and C−O bonds and shortening of the single C−C bonds, modifying the system from a quinonoid structure toward a benzenoid type of ring (1.390 Å is the C−C bond length in benzene[27]). The 1^2A_u state has an expansion of all the C−C bonds, which can be described as a ring breathing, and a contraction of the C−O bonds.

Table 4 lists the harmonic frequencies computed for the three mentioned states at the π-CASSCF level using the D_{2h} optimized geometries. Figure 2 displays some selected normal modes computed for the 1^2B_{3u} and 1^2A_u excited states. The frequencies obtained for the 1^2B_{2g} ground state can be compared to the experimental Raman and infrared (IR) determinations.[30] The CASSCF computed harmonic frequencies are overestimated by approximately 5−10%. The good performance of the CASSCF force fields in previous studies[27] to obtain vibronic intensities led us to directly use the computed frequencies and discard any scaling procedure. It is relevant to note that the computed ^2A_u force field has an imaginary frequency for the out-of-plane ν_8 a_u mode. The molecule, therefore, seems to break the planarity in the excited state. As the a_u modes will not carry much intensity on absorption from the ground state, the D_{2h} force field will be used as an effective potential in an approximate treatment of the vibrational structure of the state.[27]

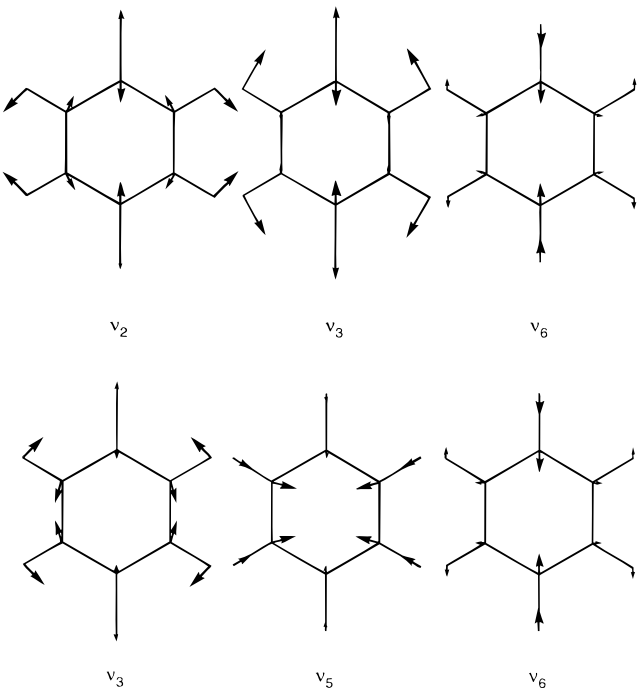

Figure 2. Computed normal modes of the 1^2B_{3u} (top) and 1^2A_u (bottom) excited states of the *p*-benzosemiquinone radical anion.

The electronic transitions from the ground state, 1^2B_{2g}, to the excited 1^2B_{3u} and 1^2A_u states are both dipole allowed for one-photon promotions. As can be expected, excitations into the symmetric modes lead to the most intense transitions of the vibronic spectra. The vibronic intensities were thus calculated by only including the totally symmetric modes, a_g, and also the b_{3u} modes, which are thermally accessible due to their low frequency. Excitations up to 2 quanta in the ground-state vibrational modes and 5 quanta in the excited-state modes were considered.

Figure 3 displays the vibronic structure of the electronic absorption transition $1^2B_{2g} \rightarrow 1^2B_{3u}$. The spectrum is a combination of fundamentals, overtones, combination, and hot bands, and exhibits a long progression of about 1 eV. Table 5 compiles the energies and oscillator strengths of the vibrational transitions. A conventional nomenclature has been introduced[44] where a mode is represented by its number and the number of quanta in the lower and upper electronic states as a subscript and a superscript, respectively.

The 0−0 transition corresponds to the most intense peak of the 1^2B_{3u} spectrum. The strongest progression carries one quanta on the ν_2 a_g mode, which has a computed harmonic frequency of 1694 cm^{-1}. The main deformations caused by this mode can be observed in Figure 2. The contributions to the composition of the mode are: 27% CCH bending, 20% C═C stretching, 20% C−C stretching, and only 14% C═O stretching. The ν_2 mode is the most efficient in bringing intensity to the bands because it is related to the geometric changes undergone by PBQ^- in passing from the ground to the 1^2B_{3u} state, that is, enlargement of both the C═C and C═O bonds and shortening of the C−C bonds. These results confirm the resonance Raman assignments[30,38,39] which attributed to mode ν_2 a_g the splitting of the peaks in the 2.7−3.1 eV region of the absorption spectrum. The first peak mostly originates in the 0−0 transition, and the second peak around 2.9 eV results from the ν_2 a_g progression with a noticeable contribution of the 3_0^1 transition

(44) Callomon, J. H.; Dunn, T. M.; Mills, I. M. *Philos. Trans. R. Soc. London* **1966**, *A259*, 499.

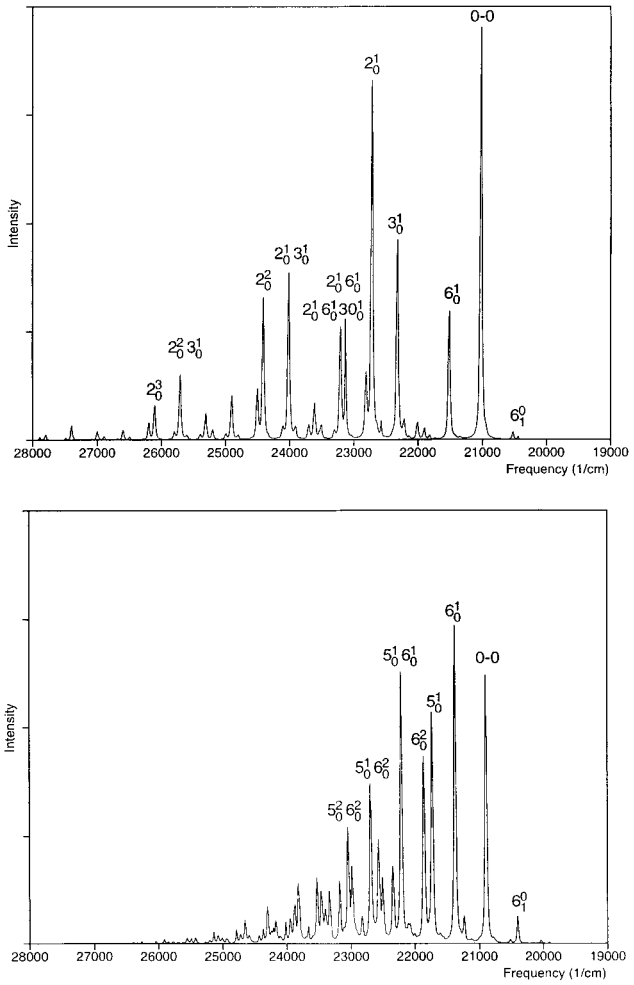

Figure 3. Computed spectra for the electron absorptions $1^2B_{2g} \rightarrow 1^2B_{3u}$ (top) and $1^2B_{2g} \rightarrow 1^2A_u$ (bottom) for the *p*-benzosemiquinone radical anion. The most important transitions are indicated. See Tables 5 and 6 for assignments.

(see Figure 3). The proposal by Harada et al.[40] that mode ν_3 a_g with larger contributions of C−O stretching (see Figure 2) is responsible for the band splitting is then not supported by our calculations, although mode ν_3 a_g also forms an intense progression in the spectrum. Another argument based on the deuterated spectrum can be added to support our interpretation. On deuteration the peak at 2.9 eV becomes sharper in the experimental spectrum.[43] The present CASSCF force field has been used to compute the vibronic band shapes of the corresponding transition for the deuterated compound (not included here for the sake of brevity). The spectrum shows a decrease of intensity for the 3_0^1 transition but not for the 2_0^1 transition, which remains the main responsible of an obviously sharper peak. Consequently, our calculations strongly support the interpretation of the two bands clearly observed in the 2.7−3.1 eV region of the absorption spectrum of PBQ^- as corresponding to a vibrational progression of the $1^2B_{2g} \rightarrow 1^2B_{3u}$ transition, and not related to the 1^2A_u state. The splitting observed between the peaks in acetonitrile, $\approx$ 1400 cm^{-1} would correspond to the computed frequency for the ν_2 mode in the 1^2B_{3u} state, 1694 cm^{-1}, a value which is overestimated in the CASSCF force field and is expected to decrease once the effects of anharmonicities and unaccuracies of the method are considered (the frequency of the ν_2 mode is overestimated by 189 cm^{-1} in the ground state, cf. Table 4). The assignment of the observed splitting to the progression on mode ν_3 can be ruled out. Such an assignment

Table 5. Computed Frequencies (cm^{-1}) and Oscillator Strengths (f) of the Main Vibronic Bands of the $1^2B_{2g} \rightarrow 1^2B_{3u}$ Transition in the *p*-Benzosemiquinone Radical Anion (PBQ^-)[a]

frequency	$f/10^{-2}$	assignment	frequency	$f/10^{-2}$	assignment
20522	0.027	6_1^0	23612	0.115	3_0^2
20999	0.099	29_1^1	23624	0.057	$3_0^2 30_1^1$
21014	0.076	6_1^1	23698	0.040	$2_0^1 6_0^2$
21021	1.443	0−0	23901	0.031	$2_0^1 4_0^1$
21033	0.715	30_1^1	24010	0.587	$2_0^1 3_0^1$
21046	0.353	30_2^2	24023	0.291	$2_0^1 3_0^1 30_1^1$
21506	0.059	6_1^2	24036	0.144	$2_0^1 3_0^1 30_2^2$
21513	0.408	6_0^1	24104	0.031	$3_0^2 6_0^1$
21525	0.202	$6_0^1 30_1^1$	24409	0.499	2_0^2
21538	0.100	$6_0^1 30_2^2$	24422	0.247	$2_0^2 30_1^1$
21898	0.041	5_0^1	24434	0.122	$2_0^2 30_2^2$
22004	0.050	6_0^2	24502	0.158	$2_0^1 3_0^1 6_0^1$
22294	0.049	$3_0^1 29_1^1$	24515	0.078	$2_0^1 3_0^1 6_0^1 30_1^1$
22316	0.708	3_0^1	24901	0.133	$2_0^2 6_0^1$
22329	0.351	$3_0^1 30_1^1$	24913	0.066	$2_0^2 6_0^1 30_1^1$
22341	0.173	$3_0^1 20_2^2$	25196	0.033	$2_0^1 3_0^1 4_0^1$
22693	0.085	$2_0^1 29_1^1$	25306	0.090	$2_0^1 3_0^2$
22708	0.062	$2_0^1 6_1^1$	25705	0.225	$2_0^2 3_0^1$
22715	1.246	2_0^1	25717	0.111	$2_0^2 3_0^1 30_1^1$
22727	0.618	$2_0^1 30_1^1$	25730	0.055	$2_0^2 3_0^1 30_2^2$
22740	0.305	$2_0^1 30_2^2$	26103	0.123	2_0^3
22808	0.196	$3_0^1 6_0^1$	26116	0.061	$2_0^3 30_1^1$
22821	0.097	$3_0^1 6_0^1 30_1^1$	26196	0.059	$2_0^2 3_0^1 6_0^1$
23200	0.048	$2_0^1 6_1^2$	26595	0.031	$2_0^3 6_0^1$
23207	0.342	$2_0^1 6_0^1$	27000	0.032	$2_0^2 3_0^2$
23219	0.170	$2_0^1 6_0^1 30_1^1$	27399	0.053	$2_0^3 3_0^1$
23502	0.042	$3_0^1 4_0^1$	27797	0.021	2_0^4

[a] $mode_{ini}^{fin}$. See text for the nomenclature of bands.

is based on the comparison to the ground-state frequency of mode ν_3, 1435 cm^{-1},[36,43] without taking into account that this value largely decreases in the excited state. The present assignments are made, however, on the basis of both vibrational excited-state frequencies and transition intensities and seem less questionable.

Figure 3 shows the vibronic structure of the electronic absorption transition $1^2B_{2g} \rightarrow 1^2A_u$. Table 6 compiles the energies and oscillator strengths of the vibronic transitions. The vibrational progressions are shorter ($\sim$0.6 eV globally) than those in the transition to the 1^2B_{3u} state. This result agrees with qualitative expectations when analyzing the changes on the relaxed geometries of the excited states with respect to the ground state, much smaller for the 1^2A_u state. The most intense peak of the computed transition corresponds to the excitation of 1 quanta into mode ν_6 a_g (6_0^1), computed at 482 cm^{-1} above the band origin. The strongest progressions involve the ν_6 a_g mode, although the ν_5 a_g mode clearly participates in the second strongest progression. The combination of modes ν_6 and ν_5 (see Figure 2) corresponds to the breathing movement suggested by the change in the geometry associated to the $1^2B_{2g} \rightarrow 1^2A_u$ absorption (see Table 3). The enhancement of the breathing modes in the resonance Raman spectrum, which would indicate the presence of the 1^2A_u state, is not detected when excited in resonance with the lowest-energy intense peak and is only clearly observed for excitations higher than 3.2 eV.[36] This is an argument to discard the presence of the 1^2A_u state at energies

Table 6. Computed Frequencies (cm^{-1}) and Oscillator Strengths (f) of the Main Vibronic Bands of the $1^2B_{2g} \rightarrow 1^2A_u$ Transition in the *p*-Benzosemiquinone Radical Anion (PBQ^-)[a]

frequency	$f/10^{-2}$	assignment	frequency	$f/10^{-2}$	assignment
20391	0.050	$6_1^0\,30_1^1$	22572	0.344	5_0^2
20405	0.105	6_1^0	22672	0.132	$5_0^1\,6_0^1\,30_2^2$
20875	0.234	30_2^2	22684	0.062	$5_0^1\,6_1^3$
20889	0.494	30_1^1	22686	0.279	$5_0^1\,6_0^2\,30_1^1$
20893	0.063	29_1^1	22701	0.589	$5_0^1\,6_0^2$
20904	1.042	0−0	22830	0.077	6_0^4
21239	0.091	$5_0^1\,6_1^0$	22975	0.127	$3_0^1\,6_0^1\,30_1^1$
21356	0.270	$6_0^1\,30_2^2$	22990	0.267	$3_0^1\,6_0^1$
21371	0.571	$6_0^1\,30_1^1$	23039	0.190	$5_0^2\,6_0^1\,30_1^1$
21374	0.072	$6_0^1\,29_1^1$	23053	0.400	$5_0^2\,6_0^1$
21385	1.204	6_0^1	23168	0.108	$5_0^1\,6_0^3\,30_1^1$
21709	0.197	$5_0^1\,30_2^2$	23183	0.227	$5_0^1\,6_0^3$
21723	0.416	$5_0^1\,30_1^1$	23342	0.187	$3_0^1\,5_0^1$
21727	0.053	$5_0^1\,29_1^1$	23406	0.083	5_0^3
21738	0.877	5_0^1	23457	0.075	$3_0^1\,6_0^2\,30_1^1$
21838	0.156	$6_0^2\,30_2^2$	23471	0.158	$3_0^1\,6_0^2$
21850	0.075	6_1^3	23521	0.111	$5_0^2\,6_0^2\,30_1^1$
21852	0.329	$6_0^2\,30_1^1$	23535	0.233	$5_0^2\,6_0^2$
21867	0.694	6_0^2	23664	0.065	$5_0^1\,6_0^4$
22190	0.228	$5_0^1\,6_0^1\,30_2^2$	23795	0.050	$3_0^1\,5_0^1\,6_0^1\,30_2^2$
22205	0.483	$5_0^1\,6_0^1\,30_1^1$	23809	0.106	$3_0^1\,5_0^1\,6_0^1\,30_1^1$
22208	0.061	$5_0^1\,6_0^1\,29_1^1$	23824	0.223	$3_0^1\,5_0^1\,6_0^1$
22219	1.017	$5_0^1\,6_0^1$	23887	0.097	$5_0^3\,6_0^1$
22320	0.060	$6_0^3\,30_2^2$	23953	0.062	$3_0^1\,6_0^3$
22332	0.050	6_1^4	24017	0.090	$5_0^2\,6_0^3$
22334	0.126	$6_0^3\,30_1^1$	24176	0.073	$3_0^1\,5_0^2$
22348	0.266	6_0^3	24291	0.063	$3_0^1\,5_0^1\,6_0^2\,30_1^1$
22479	0.051	$3_0^1\,30_2^2$	24306	0.132	$3_0^1\,5_0^1\,6_0^2$
22494	0.107	$3_0^1\,30_1^1$	24369	0.057	$5_0^3\,6_0^2$
22508	0.225	3_0^1	24658	0.087	$3_0^1\,5_0^2\,6_0^1$
22543	0.077	$5_0^2\,30_2^2$	24787	0.052	$3_0^1\,5_0^1\,6_0^3$
22557	0.163	$5_0^2\,30_1^1$	25140	0.052	$3_0^1\,5_0^2\,6_0^2$

[a] $mode_{ini}^{fin}$. See text for the nomenclature of bands.

around 2.7−2.8 eV and to assign the broad band observed at 3.3 eV to the $1^2B_{2g} \rightarrow 1^2A_u$ transition. It is worth pointing out, however, that a group of vibronic transitions corresponding to the 1^2B_{3u} band lie in the same region of the spectrum ($2_0^1\,3_0^1$ and 2_0^2, see Figure 3) and may also contribute to the 3.3 eV feature, which is more a shoulder than a clear peak.

The overall oscillator strength calculated for the $1^2B_{2g} \rightarrow 1^2A_u$ transition from its vibrational structure is 0.1930. This result contrasts with a somewhat smaller value computed for the $1^2B_{2g} \rightarrow 1^2B_{3u}$ transition, 0.1557, despite the more intense character of some of the vibrational peaks involved in the transition to the 1^2B_{3u} state. These results are consistent with those obtained for the corresponding states in the vertical calculations (see Table 2) and may explain the discrepancies observed between different spectra, where the largest oscillator strength has been attributed to the more peaking but less broad 1^2B_{3u} band. The overall picture of the spectrum suggested by the theoretical results obtained here is that the 2.7−3.3 eV region presents a superposition of transitions to two electronic states, one lower in energy and showing sharper peaks (1^2B_{3u}), which is the responsible of two clear features, and the other higher in energy and broader (1^2A_u).

The band origins for the transitions to the 1^2B_{3u} and 1^2A_u states are difficult to establish because they are very close in energy. Using the CASSCF-optimized ground- and excited-state geometries, the adiabatic CASPT2 energies obtained for the transitions from the ground to the 1^2B_{3u} and 1^2A_u states (ANO C,O[4s3p2d]/H[3s2p] basis set) were 2.61 and 2.59 eV, respectively. These values have been used to place the spectra displayed in Figure 3 and in Tables 5 and 6. The corresponding vertical (ground-state geometry) transition energies using the same method and basis set were 2.70 and 2.78 eV, respectively. The larger relaxation observed for the 1^2A_u state (0.19 eV) than for the 1^2B_{3u} state (0.09 eV) goes against expectations. The geometry changes on excitation are smaller for the 1^2A_u state, and also the computed progressions are shorter. As it has been, however, observed in previous studies,[45,46] the use of CASSCF optimized geometries in combination with CASPT2 electronic energies leads to slight overestimations of the size of the relaxation, in particular in states with small geometric changes from the ground state. The accuracy of the present results does not then allow to place unambiguously the two bands with respect to each other. On the basis of the previous arguments and the resonance Raman data, it is probable that the 1^2A_u state is placed at higher energies than the 1^2B_{3u} state, both diabatically and adiabatically. The assignment of the observed bands seems, however, clear: the 2.7−2.9 eV intense peaks correspond to vibrational progressions of the transition to the 1^2B_{3u} state, and the 3.3 eV feature is most probably a more complex combination of bands in which the 1^2A_u state is the most important contributor.

3.4. Excited States at the Geometry of Neutral *p*-Benzoquinone. Electron-scattering studies have also provided interesting information about the energy position and character of the excited states of PBQ^-.[47−53] To obtain theoretical results which can be directly compared to the experimental data reported in those studies, the low-lying excited states of PBQ^- were recalculated at the optimized geometry of the ground state of neutral PBQ. The attachment energies, that is, the energy differences between the anion states and the ground state of the neutral system, were further calculated. The CASPT2 results, together with the values obtained experimentally using the different techniques, are collected in Table 7. The weights of the different configurations in the CASSCF wave functions are indicated in Figure 1 within parentheses.

(45) Serrano-Andrés, L.; Lindh, R.; Roos, B. O.; Merchán, M. *J. Phys. Chem.* **1993**, *97*, 9360.
(46) Serrano-Andrés, L.; Roos, B. O. *J. Am. Chem. Soc.* **1996**, *118*, 185.
(47) Christophorou, L. G.; Carter, J. G.; Christodoulides, A. A. *Chem. Phys. Lett.* **1969**, *3*, 237.
(48) Collins, P. M.; Christophorou, L. G.; Chaney, E. L.; Carter, J. G. *Chem. Phys. Lett.* **1970**, *4*, 646.
(49) Cooper, C. D.; Naff, W. T.; Compton, R. N. *J. Chem. Phys.* **1975**, *63*, 2752.
(50) Cooper, C. D.; Frey, W. F.; Compton, R. N. *J. Chem. Phys.* **1978**, *69*, 2367.
(51) Allan, M. *Chem. Phys.* **1983**, *81*, 235.
(52) Allan, M. *Chem. Phys.* **1984**, *84*, 311.
(53) Modelli, A.; Burrow, P. D. *J. Phys. Chem.* **1984**, *88*, 3550.
(54) Chowdhury, S. Heinis, T.; Grimsrud, E. P.; Kebarle, P. *J. Phys. Chem.* **1986**, *90*, 2747.
(55) Heinis, T.; Chowdhury, S.; Scott, S. L.; Kebarle, P. *J. Am. Chem. Soc.* **1988**, *110*, 400.
(56) Adams, G. E.; Michael, B. D. *Trans. Faraday Soc.* **1967**, *63*, 1171.
(57) Herzberg, G. *Molecular Spectra and Molecular Structure, II*; *Infrared and Raman Spectra of Polyatomic Molecules*; Van Nostrand: New York, 1945.
(58) Wilson, E. B.; Decius, J. C.; Cross, P. C. *Molecular Vibrations*; McGraw-Hill: New York, 1955.
(59) Bauscher, M.; Mantele, W. *J. Phys. Chem.* **1992,** *96*, 11101.

Table 7. CASPT2 Attachment Energies (AE) of *p*-Benzoquinone[a]

state	AE (eV)	experimental (eV)				relative energy (eV)
		SF_6 SS[b]	ETS[c]	ETS[d]	vib. exc.[e]	
1^2B_{2g}	−1.64					0.00
1^2B_{3g}	0.87					2.51
1^2A_u	0.91	0.70	0.72	0.69	0.77	2.55
1^2B_{2u}	0.96					2.60
1^2B_{3u}	1.31	1.35	1.43	1.41	1.6	2.95
2^2B_{3u}	1.87	1.90	2.15	2.11	2.0	3.51
1^2B_{1g}	1.99					3.63

[a] The AE is the energy difference between the anion state and the ground state of the neutral molecule, both computed at the CASSCF optimized geometry of the neutral system. [b] Data from SF_6 scavenger spectra, ref 49. [c] Data from electron transmission spectroscopy, ref 51. [d] Data from electron transmission spectroscopy, ref 53. [e] Data from vibrational excitation by electron impact, ref 52.

The 1^2B_{2g} state is computed to be the lowest-energy state of the radical anion at this geometry. It is located 1.64 eV below the ground state of the neutral molecule. It has therefore undergone a destabilization of 0.37 eV with respect to the equilibrium geometry. As regards the excited states, their energetic ordering becomes completely altered upon modification of the structural parameters. This is due to the very different effect that the geometric variations have on the energy of the states. All of them become destabilized in a total energy scale, but the energy increase goes from 0.11 eV, in the case of the 1^2A_u state, to 0.76 eV for the 1^2B_{1g}. To make easier the comparison, the relative energies of the excited states of the ion with respect to the 1^2B_{2g} ground state have been included in the last column of Table 7. The 1^2B_{2u} and 1^2B_{3g} nπ* states undergo strong destabilizations. According to the CASPT2 calculations, they are placed 2.5−2.6 eV above the ground state of the anion, and the $^2B_{3g}$ state is computed to be more stable than the 1^2B_{2u} state. The corresponding excitation energies at the geometry of the anion, shown in Table 2, were in the range 2.2−2.3 eV, and the order of relative stability was the opposite.

The most significant changes occur for the 1^2B_{3u} and 1^2A_u states. They were computed to be quasi-degenerate at the optimized geometry of the anion. In contrast, at the geometry of the neutral system, they are separated by 0.40 eV, the 1^2A_u state being lower in energy. Whereas the total energy of the 1^2B_{3u} state strongly increases (0.52 eV), the corresponding value for the 1^2A_u state changes very little (0.11 eV) upon the structural modifications. Thus, the relative energy increases for the B_{3u} state (from 2.80 to 2.95 eV), but decreases for the A_u state (from 2.82 to 2.55 eV). This different behavior can be rationalized on the basis of the geometries optimized for the two states and discussed in the previous section. For the 1^2B_{3u} state, the optimized structural parameters show significant deviations from those obtained for the ground state of the anion, but the differences are much larger when compared to the computed values for the ground state of the neutral molecule. However, for the 1^2A_u state, some bond distances, such as C═O and C−C, are intermediate between those corresponding to PBQ and PBQ^- and the deviations are smaller. Consequently, the change of the geometry when passing from the ion to the neutral is expected to produce a strong destabilization on the B_{3u} state, but should not affect very much the energy of the A_u state, as it is corroborated by the theoretical results.

As far as the 1^2B_{1g} and 2^2B_{3u} states are concerned, they interchange their positions upon geometric changes. The relative energy of the B_{1g} state increases considerably, whereas it is nearly the same in the case of the B_{3u} state (cf. Tables 2 and 7).

According to the computed attachment energies, the temporary anion states of PBQ^- can be classified into three groups: the first group comprises states with AE values in the range 0.8−1.0 eV. The 1^2B_{3g} and 1^2B_{2u} nπ* states, as well as the 1^2A_u state (which is located between them), belong to this set. The second group is formed by the 1^2B_{3u} state, with a predicted AE of 1.31 eV. Finally, the attachment energy interval 1.8−2.0 eV defines the third group, which contains the 2^2B_{3u} and 1^2B_{1g} states.

As it is shown in Table 7, the experimental values obtained by means of the different techniques are very similar. Three low-energy resonances have been observed in such studies at electron energies around 0.7, 1.4, and 2.0 eV. Nevertheless, the assignments proposed differ substantially from one study to another. Cooper et al.[49] interpreted the resonances observed in their SF_6 scavenger spectra on the basis of a simple MO model. They associated the three resonances with the a_u, b_{3u}, and b_{2g} π* orbitals, respectively, on the basis of the qualitative agreement observed between the energy of the resonances and the semiempirical computed orbital energies. Nevertheless, the poor agreement obtained for the highest-energy resonance called this assignment into question and the authors did not rule out other explanations like, for example, a Feshbach resonance involving an nπ* state of PBQ.[49] This possibility had been previously suggested by Christophorou et al. to justify the resonance which they observed at 2.1 eV in their electron collision experiments.[47,48] Cooper et al.[50] later revised their assignment in the light of the optical absorption measurements. It was observed that the energy of the three most intense bands of the absorption spectrum and the relative energies of the resonances with respect to the ground state of the anion were very similar. Consequently, identical assignments to those reported in the optical study were proposed for the resonances, that is, $^2B_{3u}$,^2A_u, and $^2B_{3u}$. On the basis of the large signal intensities, Allan attributed the three lowest-energy features of the electron-transmission and electron-energy-loss spectra to shape resonances.[51] By means of the analysis of the vibrational excitations by electron impact, he concluded that the results were consistent with the previous assignment of these resonances to $^2B_{3u}$, ^2A_u, and $^2B_{3u}$ states.[52] Modelli and Burrow[53] also recorded the electron-transmission spectrum of PBQ and proposed an interpretation of the resonances by performing a simple perturbation analysis on the molecular orbital energies. The two lowest-energy resonances were adscribed to electron capture into the b_{3u} and a_u π* valence orbitals, respectively. However, the highest-energy feature could not be assigned to a π* shape resonance, and it was suggested that it might derive from a core-excited resonance. The similarity between its relative energy and the position of the most intense band of the absorption spectrum in solution led these authors to propose the same assignment as was suggested in the studies of the optical spectrum, that is, a $^2B_{3u}$ state.

According to the CASPT2 results, three electronic states are candidates for the assignment of the resonance detected around 0.7 eV, the 1^2B_{3g}, 1^2A_u, and 1^2B_{2u} states. The A_u state corresponds to a shape resonance, whereas the other two represent core-excited resonances (cf. Figure 1). The three lowest-energy signals recorded in the electron transmission spectra have been attributed to shape resonances on the basis of their spectral characteristics.[51] Therefore, the feature observed around 0.7 eV is assigned to the 1^2A_u state. With regard to the resonance at 1.4 eV, only the 1^2B_{3u} state has been computed to have an attachment energy in this range. Therefore, this is the assignment proposed. It is worth analyzing the corresponding wave function sketched in Figure 1. The weights of the

configurations calculated at the geometry of the anion and those obtained at the geometry of the neutral species do not significantly change for the states which are mainly single-configurational. However, for those states which exhibit strong configuration mixings, such as the $^2B_{3u}$ states, the weights become rather different. In the case of the first root of B_{3u} symmetry, the most important configuration is the L $\rightarrow$ $3b_{3u}$ excitation (shape character), with a computed weight of 50%, instead of the H $-$ 1 $\rightarrow$ L one-electron promotion (core-excited character), which exhibited the largest contribution to the wave function at the optimized geometry of the anion. This is in agreement with the shape character predicted experimentally for the resonance at 1.4 eV. The 2^2B_{3u} and 1^2B_{1g} electronic states are candidates for the assignment of the resonance observed around 2 eV. The latter corresponds to a Feshbach resonance. Consequently, it was excluded and the 2^2B_{3u} state was assigned as responsible for such a feature. Its CASSCF wave function exhibits a strong multiconfigurational character, with three important configurations of similar weights.

The occurrence of core-excited temporary anion states in the same regions where two resonances have been detected should be also emphasized, since they could be involved in radiationless transitions from the observed resonances and, therefore, in the dynamics of the anion. Indeed, the formation of a long-lifetime negative ion has been explained considering fast radiationless relaxation processes, which would be enhanced by the occurrence of these electronic anion states.[2,49,51]

The assignment of the resonances to the 1^2A_u, 1^2B_{3u}, and 2^2B_{3u} states (in the order of increasing energy) proposed here does not support any of the previously reported assignments. Most of them were based on the comparison with the optical absorption spectrum, which also exhibited three bands. However, the present results show the invalidity of such a procedure, since the position of the states strongly changes with the geometric modifications. Likewise, the fact that simple MO models cannot provide a full interpretation of the experimental features can be understood in the light of the strong configuration mixing observed for some relevant excited states.

4. Conclusions

We have presented results from an ab initio study of the low-lying electronic states of the *p*-benzosemiquinone radical anion. The study has been performed with multi-configurational second-order perturbation theory using the CASPT2 method. The geometry of the anion has been optimized at the CASSCF level and, compared to the neutral molecule, a more benzenoid structure has been obtained. The ground state of the anion is found to be of $^2B_{2g}$ symmetry, which corresponds to the attachment of an electron to the LUMO. The computed electron affinity is positive at the CASPT2 level and agrees with the experimental data.

The calculation of the vertical excited states enables the understanding of important features of the spectrum of the radical anion. Two Feshbach resonances (1^2B_{2u} and 1^2B_{3g}) have been found in the energy range 2.2$-$2.3 eV and have been proposed as responsible for the weak tail observed in the excitation spectrum in the same region and for the peaks detected between 2.2 and 2.5 eV in the photodetachment spectrum. The most intense band of the absorption spectrum, observed at 3.8$-$4.1 eV, has been assigned to the 2^2B_{3u} $\pi\pi^*$ state.

To provide an interpretation of the strong features detected between 2.7 and 3.1 eV and the unresolved shoulder observed around 3.3 eV, a calculation of the vibronic frequencies and intensities of the two lowest-energy intense absorption bands has been carried out. The sharp peaks at 2.7$-$3.1 eV have been attributed to the vibrational structure of the $1^2B_{2g} \rightarrow 1^2B_{3u}$ transition, due to the ν_2 a_g mode. This confirms the assignment proposed on the basis of resonance Raman measurements. Nevertheless, the $1^2B_{2g} \rightarrow 1^2A_u$ transition is found in the same region. It exhibits a larger computed oscillator strength, but it is less peaking and more broad than the 1^2B_{3u} band. Therefore, it is expected to contribute to the features observed between 2.7 and 3.4 eV. Indeed, the 3.3 eV feature has been assigned to a complex combination of bands in which the 1^2A_u state plays the major role.

The calculation of the excited states at the optimized geometry of neutral *p*-benzoquinone made possible the interpretation of the experimental data obtained with electron scattering techniques. The three resonances observed around 0.7, 1.4, and 2.0 eV have been attributed to the 1^2A_u, 1^2B_{3u}, and 2^2B_{3u} states, respectively, ruling out previous assignments based on simple MO models or comparisons to optical absorption spectra.

Acknowledgment. The research reported in this contribution has been supported by the projects PB95-0428-C02, PB98-1447, and PB97-1377 of Spanish DGES-MEC and by the European Commission through the TMR network FMRX-CT96-0079.

JA994402M